Chapter 11
CO_2 Discharged from a Compound Micro-grid of a Hydrogenation City Gas Engine and a Fuel Cell

11.1 Introduction

The introduction to a urban area of a micro-grid has the following advantages: (a) The heat transport distance is short, and effective use of the exhaust heat of the generating equipment is possible; (b) the optimal facility for the energy demand characteristic of a community is installed, and a system having small environmental impact can be built; and (c) with an independent micro-grid, the scale of equipment for distributing electricity is small [21–23]. Furthermore, (d) connecting renewable energy considering regionality is expected to become an advanced system in micro-grid technology. At present, the method of a micro-grid interconnecting with commercial power, etc., is being investigated (interconnect micro-grid) [23]. However, in order to achieve the advantages of (a)-(d) described above, it is necessary to operate a micro-grid independently. The subjects of the independent micro-grid are back-up in the case of overload and securing of power quality (voltage and frequency). Furthermore, it is necessary to clarify the power generation efficiency, the carbon dioxide emissions, and the power cost of an independent micro-grid. An improvement in power generation efficiency is expected from the independent micro-grid using a fuel cell compared with conventional electric power-supply technology. However, at the moment, fuel cells are expensive and whether they will spread is not clear. As for a fuel cell independent micro-grid, power-generation efficiency and carbon dioxide emissions are expected to be advantageous compared with existing generating equipment. However, because the fuel cell is expensive, it is difficult to install the capacity corresponding to a load peak. Consequently, there is a case of operation that limits operation of a fuel cell to a highly efficient load region [76]. The hydrogenation technology of a city gas engine is effective concerning efficiency falls and increases in carbon dioxide emission at the time of partial load operation [71–74]. The power-generation system using a city gas engine with a generator (NEG) is cheap compared with the fuel cell. Thus, this chapter examines the power-

S. Obara, *Fuel Cell Micro-grids*,
© 2009 Springer, Power Systems Series

generation efficiency and carbon dioxide emission when connecting NEG and the proton exchange membrane fuel cell (PEM-FC) to an independent micro-grid. In this chapter, the load of an independent micro-grid is divided into a base load region and a fluctuating load region, and the system that compounds NEG and PEM-FC is examined. Below, the independent micro-grid that compounds the NEG and PEM-FC systems is described as IMPE.

11.2 System Scheme

11.2.1 The IMPE Model

A micro-grid model is shown in Fig. 11.1. Figure 11.1(a) shows a system-interconnection micro-grid. This system is interconnected with commercial power, etc. Power P_c is delivered and received between other grids, and Power P_g is supplied to a micro-grid with the generating equipment installed in the machinery room of Building 5 in the urban area model of Fig. 11.1(a). The power quality (frequency, voltage) of the system-interconnection micro-grid is dependent on other grids for interconnection. Therefore, even if a large load is added to this grid, power quality is stabilized in a short time. On the other hand, Fig. 11.1(b) shows an independent micro-grid that does not interconnect with other grid systems. The method that supplies the power of an independent micro-grid by a one-set power-generation system is defined as a centralized system. Two sets of NEG or PEM-FC systems are introduced, and how to divide them into a base load operation and a fluctuating load operation, and supply power is defined as a base load-sharing system. However, the base load-sharing system corresponds to a base load and fluctuating load using either FC or NEG. For example, how to correspond base-load operation by NEG and correspond to a fluctuating-load operation by the

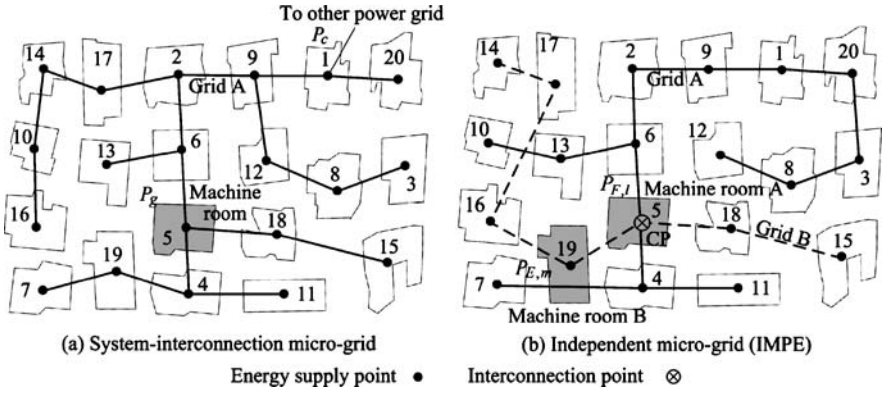

Fig. 11.1 The micro-grid model

PEM-FC system is defined as an IMPE system. By the IMPE system, the kinds of generating equipment of the base-load operation and the fluctuating-load operation differ.

11.2.2 Operation Method of the Micro-grid

Figure 11.2 shows the power load pattern of the independent micro-grid shown in Fig. 11.1(b). The load pattern of Fig. 11.1(b) is separated into a base load region and a fluctuating load region in systems other than the centralized system. As Fig. 11.1(b) shows, the PEM-FC system of capacity $P_{F,l}$ is installed in building 5 linked to Grid A, and NEG of capacity $P_{E,m}$ is installed in building 19 linked to Grid B. Grids A and B can deliver and receive the power by system interconnection equipment CP. Therefore, the PEM-FC system of building 5 is made to correspond to the base load region of Fig. 11.2, and NEG of building 19 is made to correspond to a fluctuating load region.

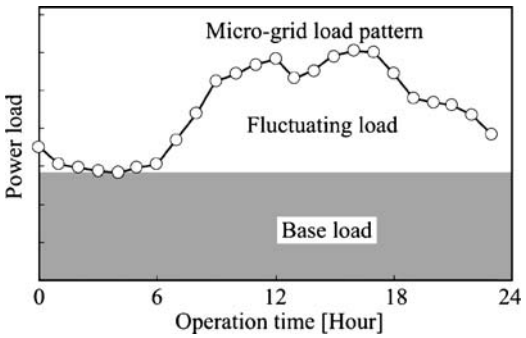

Fig. 11.2 Output share model of load power

11.2.3 Equipment Scheme

Figure 11.3 shows an example of equipment schemes of the building connected to IMPE shown in Fig. 11.1(b). Figure 11.3(a) shows the equipment scheme of Building m linked to an NEG central system. The generating equipment installed with a centralized system is any one set of FC or NEG. Figure 11.3(a) shows the equipment scheme of the central system using NEG, where NEG, a boiler, a heat storage tank, an interconnection device, etc., are installed. Although city gas (Q_E) is supplied to NEG, at the time of low load, hydrogen (Q_{Er}) is supplied through reformed gas piping. However, the equipment cost can also be reduced by installing a city gas reformer in the same building, m , as NEG. NEG and PEM-FC systems are installed in Building l ; and the equipment scheme of the IMPE system corresponding to the base load or the fluctuating load is shown in Fig. 11.3(b).

The hydrogen produced by the reformer is supplied to NEG at the time of low load, and PEM-FC stack, NEG, PEM-FC stack, a city gas reformer, a boiler, a heat storage tank, an interconnection device, etc., are installed in the building shown in Fig. 11.3(b). City gas (Q_S) is a heat source, and city gas (Q_R) produces reformed gas with the fuel for reforming. Furthermore, in order to reduce the CO concentration in the reformed gas in a fuel cell stack entrance to several ppm, a carbon monoxide oxidization section is provided. In the carbon monoxide oxidation section, carbon monoxide is burned on a catalyst and it changes into carbon dioxide. The direct current power generated by the fuel cell stack is changed into an alternating current of fixed frequency through an inverter, and is supplied to an interconnection device. Figure 11.3(c) shows the equipment scheme of Building n in which NEG or PEM-FC system is not installed. The power demand of Building n is received from a micro-grid through an interconnection device. Moreover, heat supply is obtained by city gas (Q_B) burning of a boiler. Carbon dioxide emissions are calculated from the city gas supplied to a reformer (Q_R and Q_S) and NEG (Q_E).

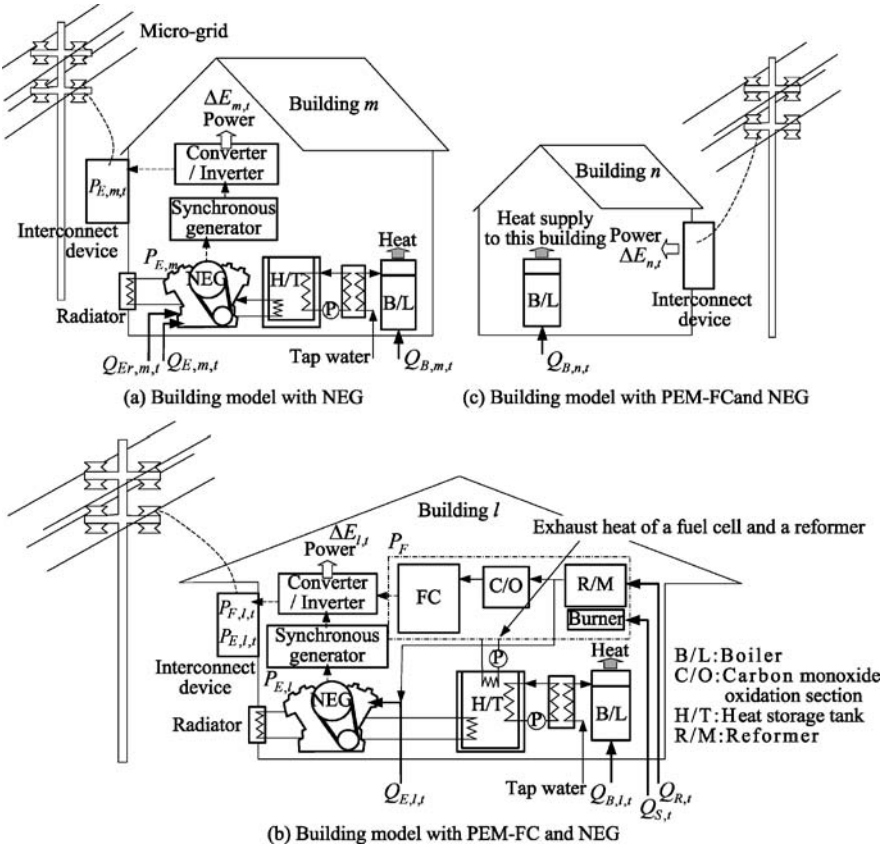

Fig. 11.3 Energy equipment model

11.3 Equipment Characteristics

11.3.1 Output Characteristics of the Gas Engine Power Generator

Figure 11.4(a) shows the examination results of the hydrogenation rate and brake thermal efficiency of a one-cylinder city gas engine [71]. The engine mean effective pressure of hydrogenation is effective in a range that is less than 0.8 MPa. Thermal efficiency with a large mean effective pressure without hydrogenation in a range exceeding 0.8 MPa can be obtained. Figure 11.4(b) shows the relation between the mean effective pressure and the brake thermal efficiency, and the hydrogenation rate [71]. The broken line in the figure is the hydrogenation rate indicating the maximum thermal efficiency. Figure 11.4(c) shows the analysis results of the production of electricity of NEG, city gas consumption, and the amount of hydrogenation calculated from the model of Figs 11.4(a) and (b). The

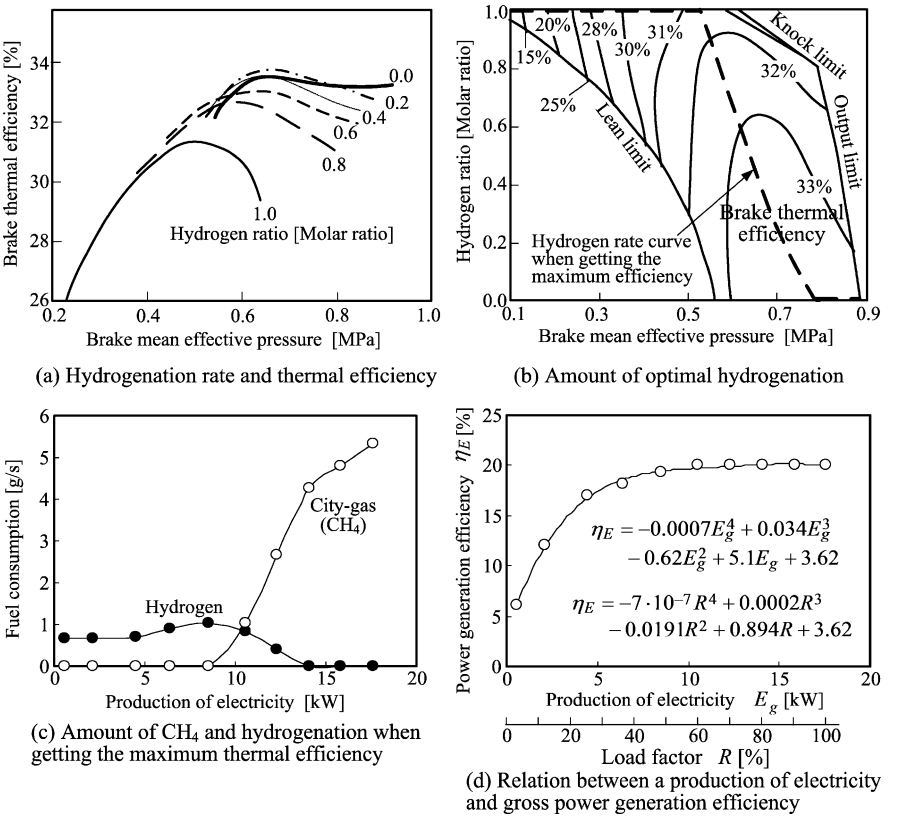

(a) Hydrogenation rate and thermal efficiency

(b) Amount of optimal hydrogenation

(c) Amount of CH_4 and hydrogenation when getting the maximum thermal efficiency

(d) Relation between a production of electricity and gross power generation efficiency

Fig. 11.4 Output characteristics of NEG

Table 11.1 Specifications of NEG

(a) Gas engine specifications

Number of cylinders	Single cylinder
Total stroke volume	1600cc
Net maximum power	88kW
Maximum brake thermal efficiency	33%
Number of revolutions	3300rpm

(b) Generator specifications

Generator type	Single-phase synchronized
Rated output	20kVA
Rated voltage	100V
Efficiency	90%
Frequency	50Hz
	Automatic voltage regulator

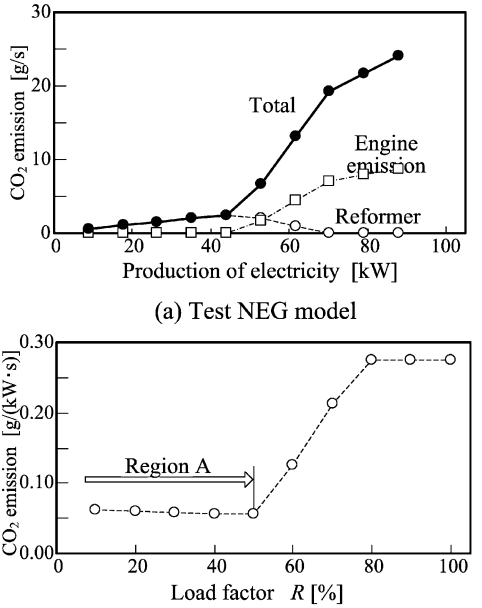

Fig. 11.5 CO_2 emission characteristics of NEG

amount of hydrogenation of Fig. 11.4(c) is the result when obtaining the maximum thermal efficiency. The specifications of a city gas engine and a power generator are shown in Tables 11.1(a) and (b). Hydrogen consumption is zero when the production of electricity exceeds 14 kW, as shown in Fig. 11.4(c). This is because high thermal efficiency can be obtained even if there is no hydrogenation in the large range of engine power, as Fig. 11.4(a) describes. Figure 11.4(d) shows the relation of the production of electricity and the generation efficiency of NEG. Although reformed gas is supplied to NEG, the generation efficiency of Fig. 11.4(d) includes reformer efficiency. The reformer is as common as the PEM-FC system described below. Details of reformer efficiency are given in the section "The PEM-FC System".

Figure 11.5(a) shows the relation between carbon dioxide emission and the production of electricity of NEG and engine hydrogenation. This model was calculated from the characteristics of the thermal efficiency described in Figs. 11.4 and

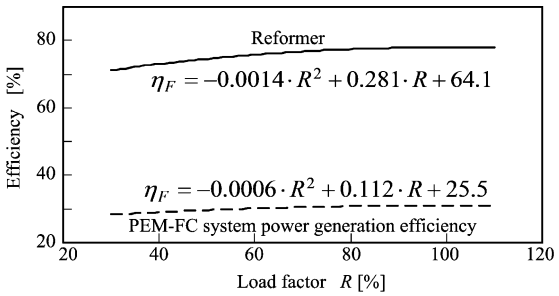

(a) Reformer efficiency and PEM-FC system power generation efficiency

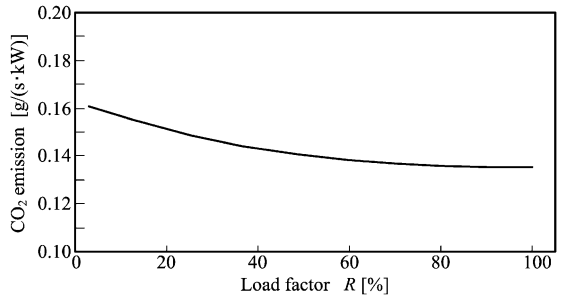

(b) CO_2 emission characteristics of PEM-FC system

Fig. 11.6 Output characteristics of the PEM-FC system

the equations (Eq. (11.1)-(11.3)) described below. The fuel supplied to NEG has many hydrogen rates in a low-load region, and there are many rates of city gas in a high-load region. Therefore, there are many rates of carbon dioxide discharged with a reforming reaction and a reformer burner in a low-load region, and there are many rates of carbon dioxide discharged by the engine burning of city gas in a high-load region. Figure 11.5(b) shows the model of a load factor and CO_2 emissions calculated from Fig. 11.5(a). In Region A in this figure, NEG is mainly operated using reforming gas. In this region, CO_2 emissions decrease slightly with the rise of a load factor. It is because reformer efficiency will improve when a load factor rises as described in the section "The PEM-FC System" and Fig. 11.6.

11.3.2 Carbon Dioxide Emissions of NEG

Equation (11.1) is a steam-reforming reaction equation of city gas (CH_4). Since this equation is an endothermic reaction, the heat for advancing its response is produced using the combustion reaction of CH_4 shown in Eq. (11.2). Moreover, Eq. (11.3) is an equation that changes the carbon monoxide of Eq. (11.1) into carbon dioxide and hydrogen. If the hydrogen quantity supplied to NEG and the

PEM-FC stack is determined, the amount of city gas supplied to a reformer and the carbon dioxide to be discharged are calculable using Eqs. (11.1)–(11.3). The CH_4 quantity supplied to an engine is calculable using Eqs. (11.2), and Figs. 11.4(a) and (b).

$$CH_4 + H_2O \rightarrow CO + 3H_2 - 206 \text{ [kJ/mol]} \tag{11.1}$$

$$CH_4 + 2O_2 \rightarrow CO_2 + 2H_2O + 802 \text{ [kJ/mol]} \tag{11.2}$$

$$CO + H_2O \rightarrow CO_2 + H_2 + 41 \text{ [kJ/mol]} \tag{11.3}$$

Equation (11.4) expresses the amount of carbon dioxide discharged by NEG. $G_{E,p,t}$ is the carbon dioxide emission when burning CH4 with engine p. $G_{R,p,t}$ is the amount of carbon dioxide discharged by a reforming reaction required for engine hydrogenation. $G_{S,p,t}$ is the carbon dioxide emission of a heat-source burner. N_R is the installed number of NEG, and in the NEG centralized system and a NEG base-load IMPE system, it is one set, and it is two sets in the NEG base load-sharing system.

$$G_{NEG,t} = \sum_{p=1}^{N_E} \left(G_{E,p,t} + G_{R,p,t} + G_{S,p,t} \right) \tag{11.4}$$

11.3.3 The PEM-FC System

Figure 11.6 shows the model of the generation efficiency of PEM-FC system and the city gas reformer efficiency [77]. Moreover, generation efficiency η_F of Fig. 11.6(a) was calculated using Eq. (11.5). When the sampling time is expressed with t, $E_{F,t}$ of Eq. (11.5), the right-hand side is the power in the inverter outlet of a PEM-FC system. $Q_{R,F,t}$ expresses the calorific power of CH_4 for reforming, and $Q_{S,F,t}$ expresses the calorific power of CH_4 supplied to a heat-source burner. The maximum generation efficiency of the fuel cell shown in Fig. 11.6 is 31%. Moreover, the reformer efficiency in Fig. 11.6(a) improves with the increase in a load factor. Figure 11.6(b) shows the CO_2 emissions of the PEM-FC system. Figure 11.6(b) shows the result of calculating based on the power-generation efficiency and reformer efficiency in Fig. 11.6(a). At the time of the hydrogen supply to the PEM-FC stack, the amount of CO_2 discharged by a reforming reaction is expressed with $G_{R,F,t}$, and the quantity discharged by a heat-source burner is expressed with $G_{S,F,t}$. Therefore, the amount $G_{F,t}$ of CO_2 discharged by the generation of the PEM-FC system is calculated by Eq. (11.6).

$$\eta_{F,t} = \left\{ E_{F,t} \Big/ \left(Q_{R,F,t} + Q_{S,F,t} \right) \right\} \times 100 \tag{11.5}$$

$$G_{F,t} = G_{R,F,t} + G_{S,F,t} \tag{11.6}$$

As Figure 11.5(b) shows, there is a large amount of CO_2 emission of NEG in a high-load zone, but there is a large amount of CO_2 emissions of a fuel cell in a low-load zone (Fig. 11.6(b)). From the difference in CO_2 emission characteristics, NEG is advantageous in the operation of a partial load, and the PEM-FC system is advantageous in steady operation at high load.

11.4 Case Study

11.4.1 The Urban Area Model

The urban area model analyzed in this chapter is shown in Fig. 11.7. The number of buildings is shown in this figure and the application for each building is shown in Table 11.2. The number of buildings of an urban area model is 20. The urban area model can consider various patterns. This chapter examines the characteristics of the carbon dioxide emission of the compound grid of NEG and the PEM-FC system from the case of Fig. 11.7.

Table 11.2 Power demand model for an urban area

	Building number
Family household (Two persons)	No. 1, 2
Family household (Four persons)	No. 3, 4, 5, 6, 7
Family household (Six persons)	No. 8, 9, 10
Apartment (Ten persons)	No. 11, 12, 13
Apartment (Twenty persons)	No. 14
Hotel	No. 15
Convenience store	No. 16, 17
Small office	No. 18
Factory	No. 19
Small hospital	No. 20

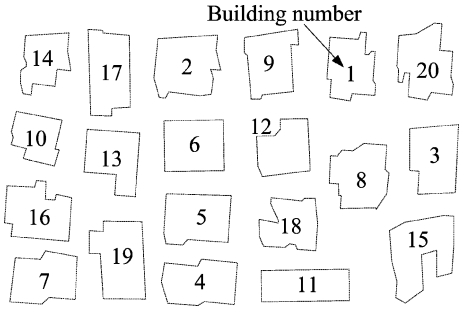

Fig. 11.7 The urban area model

11.4.2 The Power Demand Model

Figure 11.8 shows the power demand model of each building in Tokyo, and is the mean power load of each sampling time of a representative day in January (winter), May (mid-term), and August (summer) [30–33]. However, the actual power demand pattern is an assembly of the load that changes rapidly in a short time, such as an inrush current. A power demand estimate of the houses shown in Figs. 11.8(a)–(d) is difficult. On the other hand, the power demand of the small offices of Fig. 11.8(g) and the factories of Fig. 11.8(h) is regular and easy to predict. The power demand pattern of a house has a peak in the morning and in the afternoon. When midnight to early morning is excluded, hotels (Fig. 11.8(e)) have a stable demand and convenience stores (Fig. 11.8(f)) have a 24-hour power demand. In small offices (Fig. 11.8(g)), factories (Fig. 11.8(h)), and small hospitals (Fig. 11.8(i)), there is small power demand at night to early morning, and there is much power demand from morning until evening. In the case study, the CO_2 emission of August representation days, which have the largest power demand, are calculated. Figure 11.9 shows the heat demand model in August of each building described at the top of the figure [30–33]. However, in a convenience store, an office, and a factory, because the heat pump is introduced, heat demand is not taken into consideration.

11.4.3 Analysis Flow

The analysis flow of the centralized system, the base load-sharing system, and the IMPE system is shown in Fig. 11.10. First, the power demand data of each building are given to the analysis program, and the base load of the whole micro-grid is calculated. Next, the power plant capacity installed into a micro-grid is given, and the power generation efficiency and carbon dioxide emission are calculated for every sampling time concerning all the grid routes of an urban area model. By adding all these, the total power generation efficiency and the total carbon dioxide emission in the operation period, and the capacity of a power plant are determined. The load factor is calculated from the capacity and power load of a power plant. A load factor is given to the approximation of Fig. 11.4(d) or Fig. 11.6, and the power generation efficiency is determined. The carbon dioxide emission of a system are calculated by giving a load factor to the approximation of Figs. 11.5 or 11.6.

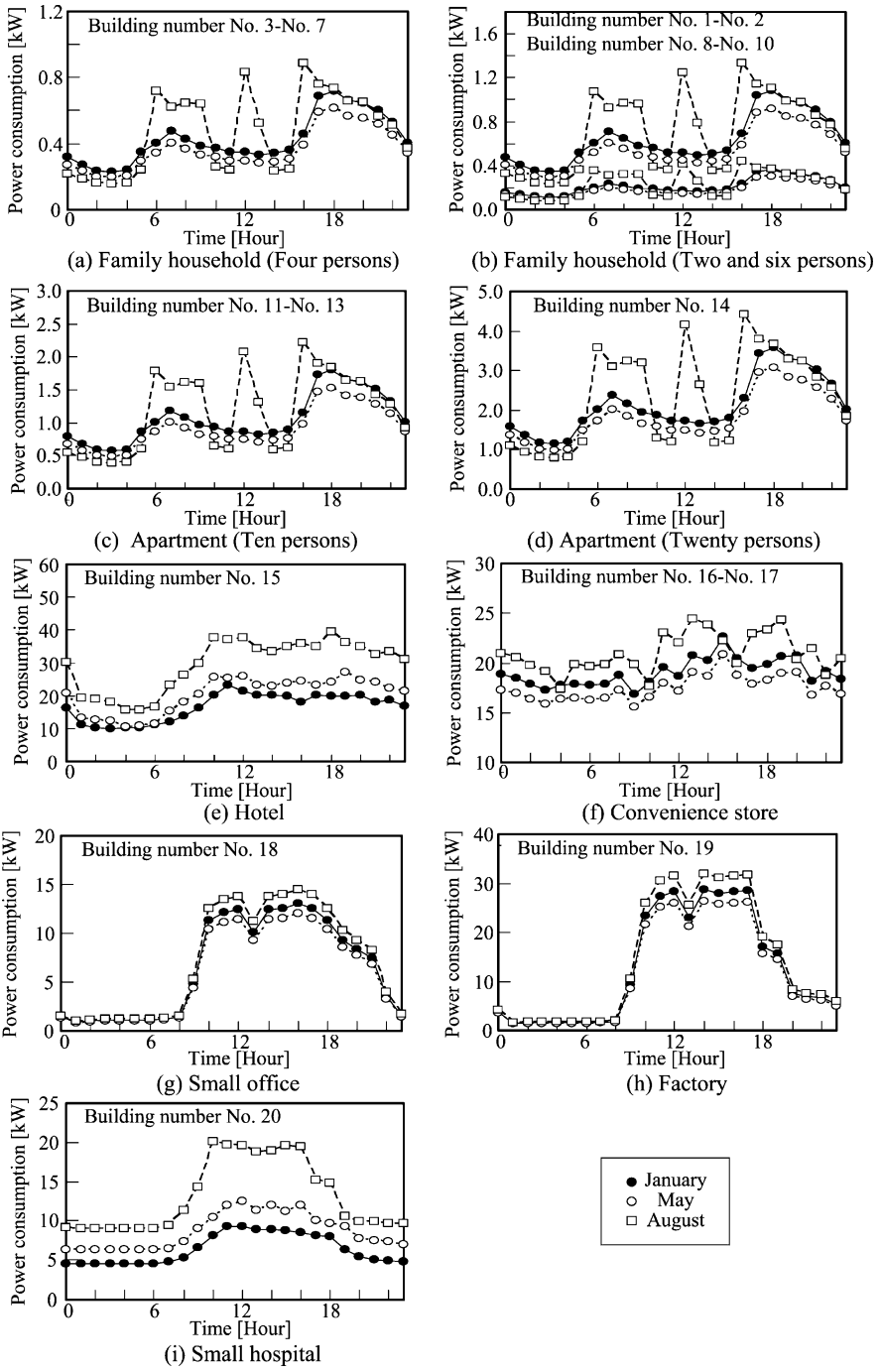

Fig. 11.8 Power demand models

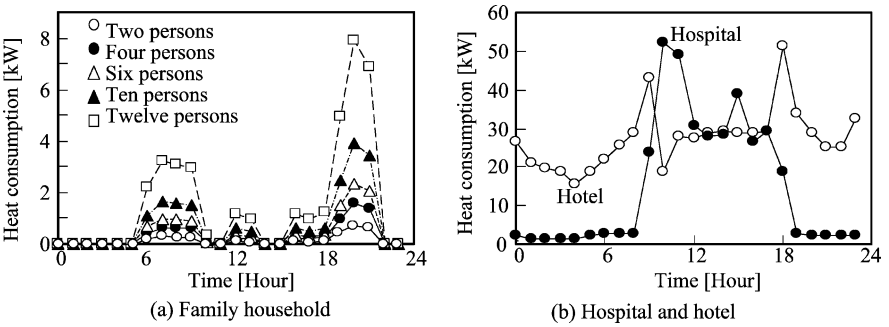

Fig. 11.9 Heat demand models in August

Fig. 11.10 Calculation flow

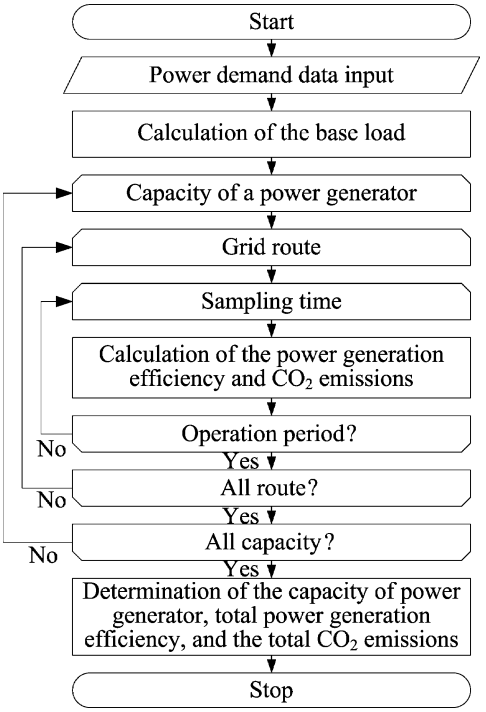

11.5 Results and Discussion

11.5.1 Power Load of the Micro-grid

Figure 11.11(a) shows the result of the power load pattern of a representative day in August of the urban area model. As the result of the time change of the power

demand, Fig. 11.11(a) shows that the power plant capacity of a fluctuating load is 100 kW, and the power plant capacity of a base load is 66 kW. Figure 11.11(b) shows the result of the rate of a base load and a fluctuating load. The base load is 1.32 times larger. Figure 11.11(c) shows the composition of the power demand added to a micro-grid. The largest load component is convenience stores (two buildings), which takes 36% of the whole load. Because there is a 24-hour power demand in convenience stores (Fig. 11.8(f)) and hotels (Fig. 11.8(e)), it is a component that smoothes the whole load added to the micro-grid. Factories and small offices of the ratio of the whole load are large. However, the demand difference during the day and at night is large, and is a component for which the fluctuating load region of a micro-grid is made to increase.

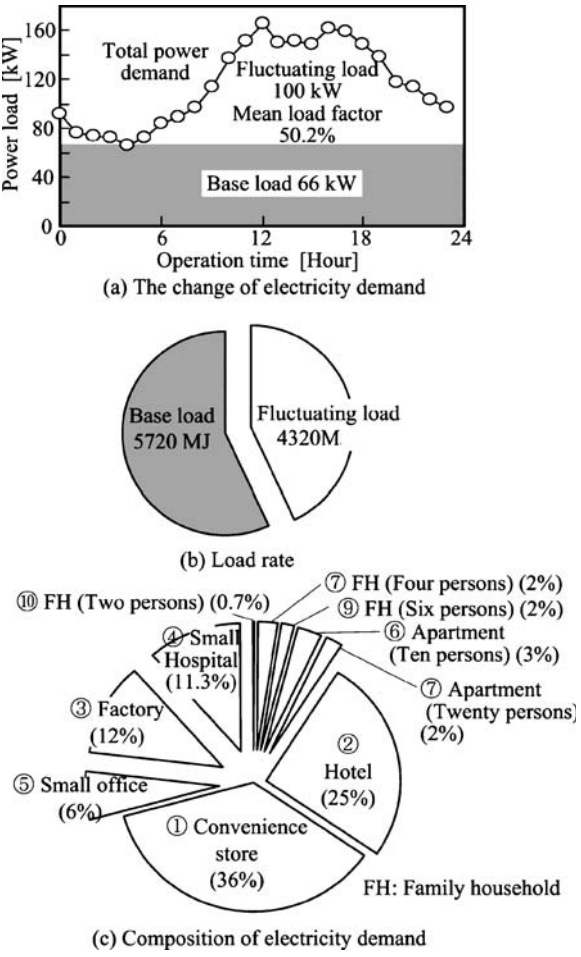

Fig. 11.11 Results of the load pattern on a representative day in May

11.5.2 Capacity of the Power Plant

The analysis results of a representative day in August are shown in Fig. 11.12. Figure 11.12(a) shows the results of the capacity of the power plant installed in each micro-grid system. (A)–(E) in Fig. 11.12 expresses the power supply method described in the figure. In a centralized system ((A) and (B)), one set of the 11.5 kW power plant is connected to a micro-grid. On the other hand, in the base load-sharing system ((C) and (D)) and the IMPE system ((E) and (F)), the power plant capacity corresponding to a base load and load fluctuation is 66 kW and 100 kW, respectively.

11.5.3 Power Generation Efficiency

Figure 11.12(b) shows the analysis results of the total power generation efficiency of the system of (A)–(F). Total power generation efficiency is high at (A), (C), (E) and (F). Most these systems are a method of corresponding to base-load operation by FC. Figure 11.12(c) shows the distribution of the power-generation efficiency of the system of (C)–(F), except for the centralized system. In FC base-load operation, it can operate at the maximum power-generation efficiency shown in Fig. 11.6(a). The maximum power-generation efficiency of PEM-FC system is higher than the efficiency of NEG shown in Fig. 11.4(d). Therefore, the total power generation efficiency of the system of (A), (C), and (E) using FC to base-load operation is high.

11.5.4 Carbon Dioxide Emissions

Figure 11.12(d) shows the analysis result of the amount of carbon dioxide discharged from each system. (C) and (E) have small CO_2 emission, and these are PEM-FC system base load operations. Moreover, (F) (NEG base load and FC load fluctuation operation) also has small CO_2 emission. When Fig. 11.5(b) is compared with Fig. 11.6(b), the change of NEG CO_2 emissions is larger than the PEM-FC system. As Figs. 11.5(b) and Fig. 11.6(b) show, when the load factor of PEM-FC system is large and the load factor of NEG is small, CO_2 emission will decrease. Therefore, there is little CO_2 emission of (C) and (E). Although (F) is the NEG base load operation, because it corresponds to load fluctuation by the large capacity PEM-FC system (100kW), there is less CO_2 emission than in the system composed only from NEG ((B) and (D)). (E') in Fig. 11.12(d) is CO_2 emission of NEG without hydrogenation. When the hydrogenation of NEG is introduced, compared with the method that does not add hydrogen, about 15% of CO_2 emission will reduce. Finally, the order with little CO_2 emission is (C), (F), (E), (E'),

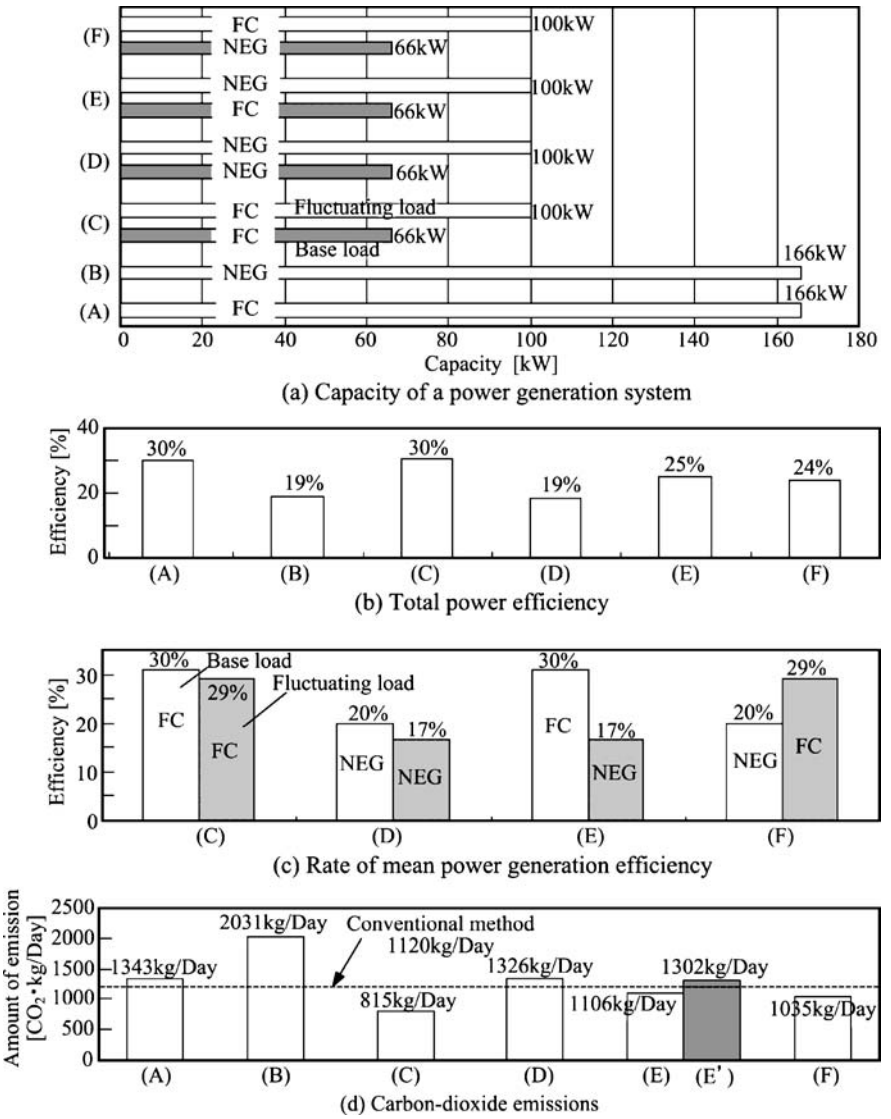

Fig. 11.12 Analysis results

(D), (A), and (B). The order ((A) and (C), (E), (F), (B) and (D)) of the power-generation efficiency described above differs from this order. Furthermore, when facility cost is taken into consideration, the smallest possible system of fuel cell capacity is advantageous. Power-generation efficiency is high, there is little CO_2 emission, and a system with cheap facility cost is the best. Therefore, system (E) is proposed in this chapter.

The energy supply by commercial power and a kerosene boiler is defined as the conventional method. The amount of greenhouse gas discharge of the conventional system is calculable based on "the investigative commission report of the calculation method of the amount of greenhouse gas discharge (the Ministry of Environment, Japan, August, 2003)". The commercial power of a greenhouse gas discharge factor is 0.331 kg-CO_2/kWh, and a kerosene boiler is set up at 0.0685 kg-CO_2/MJ, 9.5 kg-CH_4/TJ, and 0.57 kg-N_2O/TJ. As a result, as shown in Fig. 11.1(d), the CO_2 emission of system (E) decreases slightly more than with the conventional method. It depends on the amount of discharge of CO_2 on the magnitude of a power load factor. Therefore, the amounts of discharge of the system (A) differ greatly compared with the system (C).

11.5.5 Heat Demand and Exhaust Heat Output

Figure 11.13 shows the analysis results of the exhaust heat output of the base load operation and the load fluctuation operation of each system for representative days in August. The exhaust heat of each system of (A) to (F) exceeds the heat amount demanded of the urban area model in Fig. 11.7, as shown in Fig. 11.13. When an exhaust heat network is introduced into a micro-grid, and exhaust heat is distributed to each building, the boiler shown in Fig. 11.3 will become unnecessary.

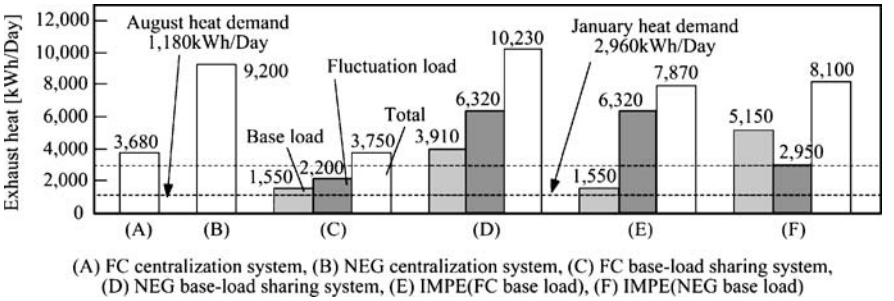

Fig. 11.13 Heat demand and exhaust heat output on representative days in August

11.6 Conclusions

Compared with the present power supply method, power-generation efficiency may improve and carbon dioxide emission may decrease in independent micro-grids using a fuel cell. However, if a fuel cell micro-grid is introduced into an urban area with great load fluctuation, it becomes a very expensive facility. Thus, for most representative days in August, this chapter examined the independent micro-grid of power demand that introduce a hydrogenation city gas engine and

the PEM-FC system, and are operated. The following conclusions were obtained as a result of installing this system into an urban area model composed from the power load patterns of 20 buildings, such as houses, offices, and hospitals.

(1) The total power generation efficiency of the centralization system, base-load sharing system, the IMPE system using PEM-FC and NEG was in the range of 19%–30%. Especially, power-generation efficiency has a high introduction of the PEM-FC system base load operation.
(2) The load factor of the PEM-FC system is large, and the system with a small load factor of NEG has little CO_2 emission. There is little CO_2 emission with the PEM-FC base-load sharing system as a result of analysis. Further, there is little CO_2 emission with the IMPE system of PEM-FC and NEG. Moreover, when hydrogen is added to NEG, CO_2 emission will be reduced by 15%.
(3) A PEM fuel cell base load and the system operating a hydrogenation city gas engine in a load fluctuation region are the most advantageous under the overall evaluation of facility cost, power generation efficiency, and CO_2 emissions. When the urban area model was analyzed using the highest system of an overall evaluation, 25% of power-generation efficiency and CO_2 emissions were 1,106 kg/day. The amount of CO_2 emission is influenced by the magnitude of the power-demand fluctuation (load factor) of the micro-grid.

The maximum effect is expected by reflecting making an energy-demand characteristic in the planning of a micro-grid. The relation between the locality of an energy demand characteristic and the optimal design of a micro-grid will be investigated hereafter.